Materials Advances

ROYAL SOCIETY OF CHEMISTRY

PAPER

View Article Online
View Journal | View Issue

Check for updates

Cite this: *Mater. Adv.*, 2021, 2, 5986

A facile, cost-effective, rapid, single-step synthesis of Ag–Cu decorated ZnO nanoflower-like composites (NFLCs) for electrochemical sensing of dopamine†

Srikanth Ponnada, [a] Demudu Babu Gorle, [b] Maryam Sadat Kiai, *[c] Saravanakumar Rajagopal, [d] Rakesh Kumar Sharma *[e] and Annapurna Nowduri *[a]

Received 9th April 2021,
Accepted 23rd July 2021

DOI: 10.1039/d1ma00319d

rsc.li/materials-advances

For clinical biology, the ability to detect neurotransmitters in the human serum environment quickly, highly sensitively, and selectively is essential. Dopamine system dysfunction has been linked to a variety of nervous system diseases. As a result, its sensitive and selective detection is critical for the early diagnosis of diseases associated with excessive dopamine levels. So, platforms for sensitive and selective monitoring of dopamine concentrations are critically needed. In this study, we synthesized a facile flower-like nanocomposite material that is cost-effective and involves a rapid single-step synthesis of an Ag–Cu decorated ZnO nanoflower-like composite (Ag–Cu@ZnO-NFLC) with a high active surface area for comparison. Ag decorated ZnO (Ag@ZnO) and Cu decorated ZnO (Cu@ZnO) were synthesized and characterized by XRD, FTIR, and Raman spectroscopy analyses. By using methods such as cyclic voltammetry, differential pulse voltammetry (DPV), and amperometry, the electrochemical behavior of a GCE modified with a single-step synthesized Ag–Cu decorated ZnO nanoflower-like composite electrode material showed promising results with an ultra-low detection limit of 0.21 μM and a high sensitivity of 0.68 μA mM^{-1} cm^{-2} by employing differential pulse voltammetry (DPV). The dopamine sensor was also tested for current densities at different pH levels, and it exhibited good stability and reproducibility. Finally, the prepared sensor was used to monitor real-time human urine samples, yielding excellent results. The findings revealed that in actual sample analysis, the as-prepared sensor showed substantial promising results in detecting dopamine.

Open Access Article. Published on 28 July 2021. Downloaded on 7/28/2025 10:24:16 PM.
This article is licensed under a Creative Commons Attribution-NonCommercial 3.0 Unported Licence.

1. Introduction

Dopamine (DA) is a neurotransmitter that belongs to the families catecholamine and phenethylamine, usually found in the nervous system, kidneys and cardiovascular system of mammals.[1] Lower or abnormal concentrations of dopamine in the blood lead to malfunctioning of kidneys and heart, and serious diseases like Parkinson's, schizophrenia, *etc.* Hence, there is a severe necessity for detecting dopamine concentrations in diagnostic practices.[2] To date, several research groups have reported many strategies and employed different techniques to detect dopamine such as chromatography, capillary electrophoresis,[3] surface-enhanced Raman scattering[4] and high-performance liquid chromatography (HPLC).[5] All of these methods require a standard experimental setup and are not cost-effective. However, in order to overcome these limitations, electrochemical detection[6] and synthesis of nanomaterials[45] has emerged and been reported by various research groups due to its low cost, simple experimental setup, sensitivity, and a wide range of materials available for modifying the electrode surface; typically, a glassy carbon electrode is used and the surface is modified by nanomaterial-like metal oxide composites including Au,[7] CuO,[8] Ag,[9] ZnO,[10] *etc.* Metal–organic frameworks (MOFs)[11,47] are widely employed because of their high electron mobility, morphological variety, and ease of synthesis.

ZnO has been in the spotlight for a decade due to its promising catalytic activity, cost effectiveness, high surface area, nontoxicity, and bio-affinity. As a result, ZnO-based

[a] *Department of Engineering Chemistry, Andhra University College of Engineering (A), Andhra University, Visakhapatnam-530003, India. E-mail: dr.nannapurna@andhrauniversity.edu.in, koolsreekanth@gmail.com*
[b] *Materials Research Centre, Indian Institute of Science, Bengaluru-560012, India*
[c] *Nano-Science and Nano-Engineering Program, Graduate School of Science, Engineering and Technology, Istanbul Technical University, Istanbul-34469, Turkey. E-mail: maryamskiai@gmail.com*
[d] *Department of Chemistry, Thiagarajar College of Engineering, Madurai, Tamil Nadu-625005, India*
[e] *Sustainable Materials and Catalysis Research Laboratory (SMCRL), Department of Chemistry, Indian Institute of Technology Jodhpur, Karwad, Jodhpur-342037, India. E-mail: rks@iitj.ac.in*

† Electronic supplementary information (ESI) available. See DOI: 10.1039/d1ma00319d

© 2021 The Author(s). Published by the Royal Society of Chemistry

Open Access Article. Published on 28 July 2021. Downloaded on 7/28/2025 10:24:16 PM.
This article is licensed under a Creative Commons Attribution-NonCommercial 3.0 Unported Licence.

nanomaterials are being used extensively in recent developments to fabricate electrochemical sensors. Cu-doped single-phase ZnO plates were synthesized *via* the hydrothermal method and have been employed for the electrochemical detection of dopamine, which showed promising performance.[12] Ionic medium supported reduced graphene oxide (im-rGO) has been reported for the electrochemical sensing of dopamine;[13] DNA electrochemical sensing *via* Ag nanoparticles decorated on carbon nanocubes has been reported for the electrochemical sensing of H_2O_2;[14] Ag@ZIF-67/GCE has been reported for the electrochemical sensing of H_2O_2.[15] Nanoparticles (NPs) of metals have been identified as potential candidates in bio-sensing. Ag nanoparticles are employed in electrochemical detection because of their low oxidation potential.[16] Cu, on the other hand, is studied extensively for various applications such as selective oxidation,[17] photocatalysis,[18] and electrochemical sensing.[18,19] Due to its great electron mobility and wide bandgap, ZnO is employed in electrochemical sensing.[18–20] Xuan Zhang *et al.* used a GCE modified with a reduced graphene oxide/ZnO nanocomposite and reported that the presence of ZnO in rGO showed an enhanced active surface area due to the versatile nature of ZnO, which in turn enabled the high sensing activity towards dopamine, uric acid, and ascorbic acid.[21]

By using a chiral ligand such as L-cysteine, chiral ZnO nanoparticles were prepared and the average particle size ranged from about 4.5 ± 1.1 nm. These chiral ZnO nanoparticles exhibited promising electrochemical behavior.[22]

The interference of ascorbic acid and uric acid was suppressed during the detection of dopamine when the novel porous rGO encapsulated ZnO microspheres were employed as surface modifiers for glassy carbon, which is a working electrode. The P-rGO acted as a Schottky barrier by suppressing the interference of AA and UA.[25] Azam Anaraki Firooz *et al.* reported that Cu-doped ZnO nanostructures modified with a GCE showed excellent electrochemical activity towards dopamine sensing.[26] Cu is reported to be an excellent catalytic material with high tunability and stability. In other experiments, Au–ZnO nanoparticles were used, which required precious high-cost Au and a longer synthesis time,[27] or ZnO sensor synthesis using microwave aided synthesis.[29] The dropping technique was used by Xiaowei *et al.* to test the dopamine (DA) sensing ability of carbon/ZnO microfibers. With a detection limit of 0.106 M, the suggested sensor demonstrated high selectivity, repeatability, and stability. Carbon/ZnO-GCE showed reduced over-potential, reduced potential difference, and increased peak currents at 0.191/0.238 V, demonstrating the improved catalytic actions of carbon/ZnO microfibers toward DA.[28] Because hollow carbon spheres have been shown to have high surface area and great mass mobility properties, and Ag particles have been shown to have great bio-affinity, high electron mobility, and prominent catalytic reactions, recently, Xinjin Zhang *et al.* synthesized Ag nanoparticle-decorated mesoporous hollow carbon spheres. As a result, the synthesized Ag-HCS/GCE showed a wide linear range and high sensitivity.[30] Recently, for the ultrasensitive detection of dopamine (DA), an electrochemical sensor based on Ag nanoparticles anchored onto CuO porous nanobelts (Ag/CuO PNBs) has been developed by Gang Liu *et al.* DA was produced by a simple two-step cation-exchange procedure followed by *in situ* thermal conversion. The anchoring Ag NPs play a large catalytic role in the redox process, and the Ag/CuO PNBs are porous structures with more active sites.[31]

Table 1 depicts the comparison of different ZnO-based nanomaterials in the electrochemical sensing of dopamine. In this study, we synthesized both Ag and Cu metals in a single step to take advantage of their known characteristics, such as bio-affinity and selectivity towards dopamine, and ZnO's high electron mobility and narrow bandgap. This method suggested a cost-effective facile Ag–Cu decorated ZnO nanoflower-like composite (NFLC) material which involved a rapid hydrothermal synthesis.

The resultant sensor exhibited high sensitivity and selectivity towards the detection of dopamine at room temperature without any further interference.

2. Experimental section

2.1. Materials and chemicals used

Copper nitrate ($Cu(NO_3)_2$), silver nitrate ($AgNO_3$), zinc nitrate ($Zn(NO_3)_2$) and ammonium hydroxide (NH_4OH) were purchased from Sigma Aldrich, India. Ethanol and acetone were procured from Himedia Laboratory Pvt. Ltd, Mumbai, India. Caffeic acid, uric acid, β-endorphin, ascorbic acid, histamine, trypramine, phenethylamine, serotonin and acetylcholine were purchased from Alfa-Aesar. All reagents and solvents were purchased from Sigma-Aldrich and Alfa Aesar and used without further purification.

Table 1 Comparison of ZnO-based electrode materials for electrochemical sensing of dopamine

S. no.	Electrode/nanomaterials	Analyte	LOD (μM) (S/N = 3)	Sensitivity (μA mM^{-1} cm^{-2})	Linear range (μM)	Detection method	Ref.
1	ZnO/CuO nanohybrid structures	Dopamine	1.0×10^{-3} and 8.0	90.9	1.0×10^{-3}–8.0 μM	CV	19
2	rGO–ZnO/GCE	Dopamine	0.33	—	1–70 μM	DPV	20
3	Chiral ZnO nanoparticles-L cysteine.	Dopamine	0.791	—	—	—	21
4	DA-imprinted CS film/ZnO NPs @C/3D-KSC	Dopamine	0.39	757	0.12 nM–152 μM	CV	22
5	ZnO nanofibers/carbon fibers	Dopamine	0.402	—	6–20 μM	DPV	23
6	P-rGO/ZnO microspheres	Dopamine	—	1240.74	1–600 μM	SWV	24
7	Cu doped ZnO (Cu/ZnO)	Dopamine	0.055		0.1–20 μM	DPV, CV	38
8	Au–ZnO NCAs/GF	Dopamine	0.04	6.23	0–80 μM	CV	39
9	**Ag–Cu decorated/ZnO nanoflower-like composite**	**Dopamine**	**0.21**	**0.68**	**0.1–10 μM**	**Amperometry**	**This work**

Open Access Article. Published on 28 July 2021. Downloaded on 7/28/2025 10:24:16 PM.
This article is licensed under a Creative Commons Attribution-NonCommercial 3.0 Unported Licence.

2.2. Synthesis of Ag–Cu decorated ZnO nanoflower-like composites (NFLCs)

The Cu/ZnO nanocomposite was prepared by a single-step hydrothermal method, in which an aqueous solution of 0.5 M zinc nitrate (Zn (NO_3) $2.6H_2O$) (Sigma Aldrich) and 0.05 M copper nitrate (Cu $(NO3)_2$) (Sigma Aldrich) was mixed with constant stirring for about 1 hour at ambient temperature. A pH value of 9.5 was maintained by gradually adding a few drops of ammonium hydroxide. The resultant solution was then transferred into a Teflon-lined autoclave followed by vigorous stirring for 30 min. Henceforth, the autoclave was sealed and heated up to 180 °C for 6 h. The final product was washed several times with ethanol and deionized water (DI) and dried at 60 °C in a hot air oven overnight. The Ag/ZnO nanocomposite was prepared through a single-step hydrothermal method, where an aqueous solution of 0.5 M zinc nitrate ($Zn(NO_3)_2{\cdot}6H_2O$) (Sigma Aldrich) and 0.05 M silver nitrate ($AgNO_3$) (Sigma Aldrich) was mixed with constant stirring for 1 hour at ambient temperature. A pH value of 9.5 was maintained by adding ammonium hydroxide into the solution drop-by-drop steadily. The resultant solution was then transferred into a Teflon-lined autoclave and stirred vigorously for 30 min. Henceforth, the autoclave was sealed and heated up to 180 °C for 6 h. The final product was washed several times with ethanol and deionized water (DI) and dried at 60 °C in a hot air oven overnight.

The Ag–Cu decorated zinc oxide nanoflower-like composite was made in a single step by mixing an aqueous solution of 0.5 M zinc nitrate (Zn (NO_3) $2.6H_2O$), 0.05 M silver nitrate (AgNO3), and 0.05 M copper nitrate Cu $(NO_3)_2$ for 1 hour at room temperature. A pH value of 9.5 was maintained by adding a few drops of ammonium hydroxide into the solution drop-by-drop very slowly. The resultant solution was then transferred into a Teflon-lined autoclave followed by vigorous stirring for 30 min. After this, the autoclave was sealed and heated up to 180 °C for 6 h. The final product was washed several times with ethanol and deionized water (DI) and dried at 60 °C in a hot air oven overnight. The XRD, XPS, FT-IR, Raman, EDAX and FE-SEM analyses were conducted to study the elemental composition and morphology of the synthesized samples.

2.3. Characterization and electrochemical techniques

FT-IR analysis was carried out using a Bruker Tensor 27 (Optik GmbH) with an RT DLaTGS (Varian) detector. The powder X-ray diffraction (PXRD) patterns were recorded at room temperature (RT) using a RigaKu SmartLab guidance instrument using copper (rotating anode) with an X-ray power of 200 ma, 45 KV (9 kW), detector's scintillation counter (0D), and D/tex(1D) HyPix-3000 (hybrid pixel array detector (2D)). The powder diffraction covered the angle ranges from 10° to 90°, with a step angle of 6° min^{-1}. The Raman spectra were recorded using a high-resolution Renishaw Raman microscope employing a He−Ne laser of 18 mW at 633 nm. The morphological structures of the prepared samples were captured using a scanning electron microscope (SEM) of TESCAN VEGA 3 with a Bruker detector. The high-resolution XPS spectra of the as-synthesized samples were recorded using a Theta Probe AR-XPS system. Cyclic voltammetry was carried out on a Biologic SP-150 workstation at room temperature in a standard three-electrode cell, where the working electrode was a glassy carbon (GC) (area = 0.07 cm^2) or modified glassy carbon, and the counter electrode was a Pt wire. The reference electrode used was the Ag/AgCl/KCl (3 M) electrode.

2.4. Electrochemical measurements

Fine alumina powder having a diameter of 0.05 and 0.3 μM was used to polish the surface of the glassy carbon electrode (GCE). The GCE was pre-treated before the surface modification, as per the procedure mentioned in the above section. Preceding the fabrication of Ag–Cu@ZnO-NFLC modified GCE, the GCE was dried at room temperature and nitrogen gas was purged continuously for half an hour. Later, 10 μL of Ag@ZnO, Cu@ZnO and Ag–Cu@ZnO-NFLC were suspended in 100 μL of ethanol and sonicated for 20 min. By using the drop casting method, the subsequent blend (3 μL) was drop cast onto the surface of the GCE. And then, the modified electrode was cleaned four times with DD water and ethanol to eliminate the unbound nanocomposite materials.

3. Results and discussion

3.1. Physical characterization of Ag–Cu decorated ZnO NFLC

The FTIR spectrum of the Ag–Cu decorated ZnO composite was recorded in the range of 400–4000 cm^{-1}, and is shown in Fig. 1A. FTIR spectroscopy provides useful information about various functional groups and metal-oxide bonds present in the composite. A significant vibration band obtained at 509 cm^{-1} corresponds to the characteristic stretching mode of the Zn–O bond. Two broad peaks at 3542 cm^{-1} (stretching) and 1280 cm^{-1} to 1470 cm^{-1} (bending) indicate the presence of an O–H functional group which is due to the absorption of atmospheric moisture on the surface of the composite.[41–43] To further confirm the components of the composite, Raman analysis was conducted as shown in Fig. 1B. Two peaks are detected at 60 cm^{-1} and 254 cm^{-1} for Cu and Ag with enhancement in the intensity, which is considered as evidence for the formation of Ag–Cu alloy nanoparticles. The main E2 mode of ZnO is clearly visible along with the Raman peaks of Ag and Cu, confirming the presence of Ag–Cu and ZnO in the NFL composite. A weak intensity peak is detected at 430 cm^{-1} in ZnO particles. The low peak of ZnO may be because its surface area is decorated with the Ag–Cu alloy, so the Raman peak intensity is relatively low. Fig. 1C shows the XRD spectrum of the Ag–Cu@ZnO NFLC. The diffraction peaks observed at 2θ = 38.34, 44.31 and 64.65 are assigned to the (111), (200) and (220) crystal planes, respectively, of the face-centred cubic phase of Ag. The peak positions match the PDF file for Ag (PDF: 01-089-3722). The diffraction peaks observed at 2θ = 43.51 and 51.57 are assigned to the (111) and (200) crystal planes, respectively, of the face-centred cubic phase of Cu. The peak position matches the PDF file for Cu (PDF: 01-085-1326).[30] However, the diffraction peaks observed at 2θ = 32.27, 34.10, 36.50, 46.40, 55.25, 62.12 and 77.72 correspond to the (100), (002), (101), (102), (110), (103) and (202) crystal planes, respectively, and the hexagonal

© 2021 The Author(s). Published by the Royal Society of Chemistry

Open Access Article. Published on 28 July 2021. Downloaded on 7/28/2025 10:24:16 PM.
This article is licensed under a Creative Commons Attribution-NonCommercial 3.0 Unported Licence.

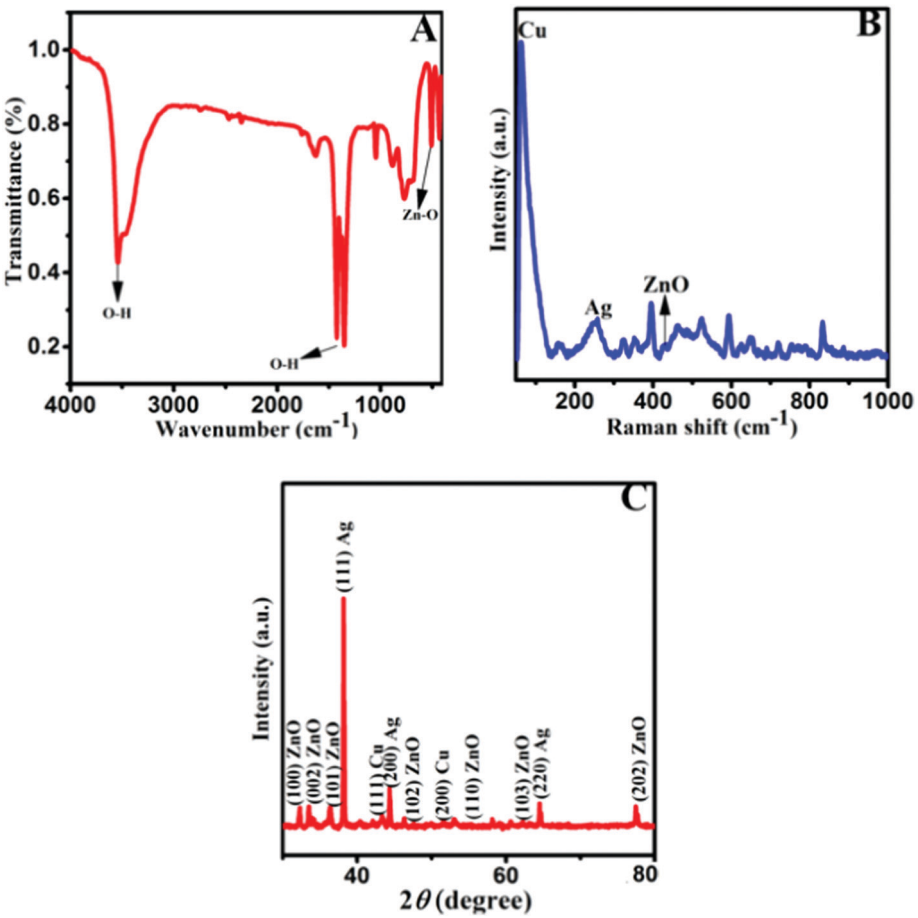

Fig. 1 (A) FTIR spectrum, (B) Raman spectrum, and (C) XRD pattern.

crystal geometry of ZnO (JCPSD card no. 01-007-2551).[44] Fig. 2A represents the SEM images of the Ag–Cu decorated ZnO composite having a nanoflower-like morphological structure with different magnifications.[32] The energy-dispersive X-ray spectrum (EDX) reveals the presence of Cu, Ag, Zn, and O elements in the stoichiometric ratio as tabulated in Fig. 2B.

The XPS analysis of the nanoparticles reveals the oxidation states of the metallic species. The structural composition of Ag–Cu decorated ZnO nanoflowers was further characterized by the XPS technique. Fig. S1 (ESI†) shows the XPS survey spectra of the Ag–Cu decorated ZnO nanoflowers, indicating the presence of constituted elements (Ag, O, Cu, and Zn). Fig. 3A shows that the $Ag3d_{5/2}$ (368.2 eV) and $Ag3d_{3/2}$ (374.5 eV) peaks are associated with 0-valent Ag at 368 and 374 eV, respectively. Besides, the good symmetry of the peaks proves that the valence of Ag does not change after the formation of the alloy with Cu. The composite shows the core-level and shakeup satellite lines of Cu 2p, as shown in Fig. 3B. In the XPS spectra (Fig. 3B), two Cu peaks at the binding energies of 934.1 and 951.3 eV were observed, which corresponded to $Cu2p_{3/2}$ and $Cu2p_{1/2}$, respectively, demonstrating the successful production of Cu nanoparticles. The existence of CuO (934.8 and 951.8 eV) along with the satellite peaks at 941.5 eV and 944.3 eV indicated that the copper on the surface region could be easily oxidized at room temperature.[33–36]

Fig. 3C shows the high-resolution XPS spectra of Zn 2p. The two symmetric signal peaks are formed at 1029.3 eV and 1052.6 eV, which corresponded to Zn $2p_{3/2}$ and Zn $2p_{1/2}$, respectively, and the energy interval between the peaks is ~23 eV. The above information confirms that Zn is completely oxidized and is in the +2 valence state. Fig. 3D illustrates the high-resolution spectra of O 1s. The peak appeared at 532.7 eV corresponding to the presence of the Zn–O bond in the ZnO structure.[46]

3.2. Electrochemical performance of Ag@ZnO, Cu@ZnO and Ag–Cu@ZnO NFLC/GCE towards dopamine detection

The nanocomposite materials were drop cast onto the GCE and their electrochemical performance was investigated using the cyclic voltammetry (CV) technique. For comparison, a bare GCE was also included as shown in Fig. 4a, which displays the CV current responses of GCE, Ag@ZnO, Cu@ZnO and Ag–Cu@ZnO-NFLC in 0.1 M PBS (pH 7.0) containing 100 μM DA at a scan rate of 50 mVs^{-1}. However, in the bare GCE, the GCE surface modified with the Ag@ZnO and Cu@ZnO nanocomposites shows no crystal-clear electrochemical response to the oxidation of DA. However, the GCE surface modified with the Ag–Cu@ZnO nanoflower-like composite exhibited an apparently strong reversible peak, that is, one anodic peak at 0.24 V and one cathodic peak at 0.005 V with high peak

Open Access Article. Published on 28 July 2021. Downloaded on 7/28/2025 10:24:16 PM.
This article is licensed under a Creative Commons Attribution-NonCommercial 3.0 Unported Licence.

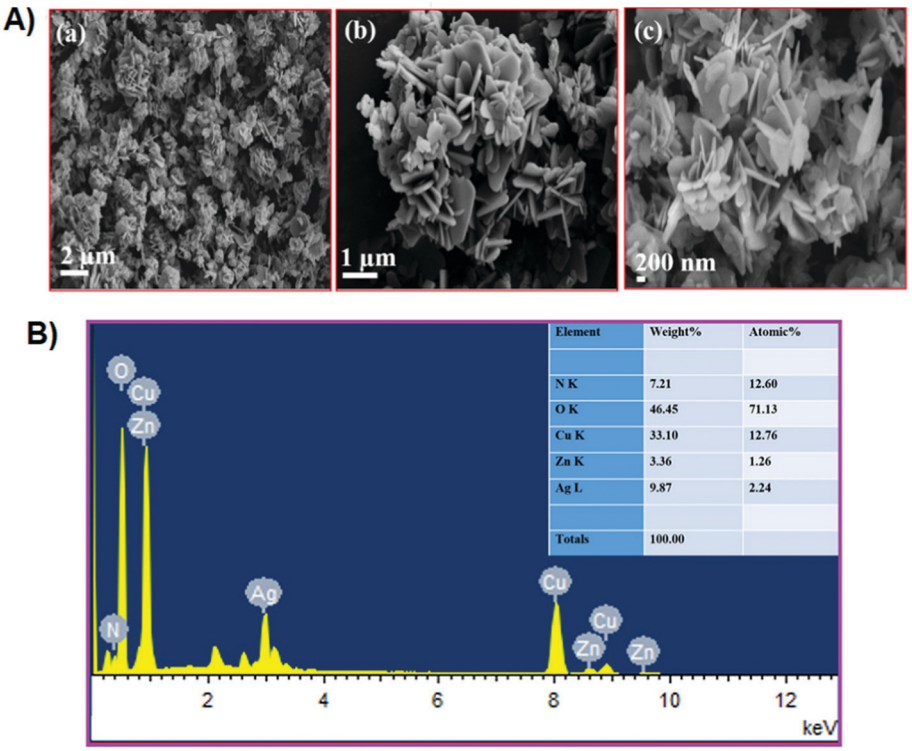

Fig. 2 (A) SEM images of Ag–Cu@ZnO NFLC. (B) EDX spectra of the Ag–Cu decorated ZnO-NFLC material; the inset shows the EDX wt% of Ag–Cu decorated ZnO-NFLC material.

currents. However, the exceptional increase in the redox peak currents at the Ag–Cu@ZnO-NFLC/GCE with a competently characterized redox couple of dopamine can be allocated to its higher electrocatalytic activity when compared with the GCE and Ag@ZnO and Cu@ZnO nanocomposite samples. Perhaps, the enhanced electrocatalytic activity is due to its association with the synergic action between the Ag support and Cu NPs on the increased surface area of the ZnO electrode surface.

The anodic current at the Ag–Cu@ZnO-NFLC/GCE increased significantly and the well-defined oxidation and reduction waves were recorded. In addition, the stronger oxidation response measured at the composite Ag–Cu@ZnO-NFLC/GCE electrode seems to imply that this material creates a favorable microenvironment for dopamine oxidation, which might be related to the composite electrode's higher surface area and better electron transfer rate.

Apart from this, the Ag–Cu nanocomposite material provides enhanced support for the adsorption of DA and also helps in the mobility of the electrons between the GCE and the analyte, henceforth exhibiting a remarkable increase in the electron transfer rate. The mechanism of electrochemical oxidation of dopamine on the Ag–Cu@ZnO-NFLC/GCE surface is depicted in Scheme 1 by the exchange of two protons and two electrons between the DA and electrochemically oxidized molecules.

When dopamine hydrochloride is subjected to a ramping potential of −0.3 V to +0.5 V *vs.* Ag/AgCl, the transfer of electrons from the NFLC material to the GCE results in an increased faradaic current. Henceforth, an optimizated pH value of 7.0 was identified from the CV current responses for 100 μM DA on Ag–Cu@ZnO-NFLC/GCE in 0.1 M PBS.

3.2.1. Studies on the effect of scan rates (sweep rates). Fig. 4b depicts the CV to understand the effects of various sweep rates ranging from 10 to 100 mV s^{-1} on the redox behavior of 100 μM DA at Ag–Cu@ZnO-NFLC/GCE in 0.1 M PBS (pH 7.0). The CV of the Ag–Cu@ZnO-NFLC/GCE shows three well-resolved peaks (Fig. 4b). As shown in Fig. 4b, increasing the scan rate causes an increase in both the oxidation and the reduction peak currents, as well as a slight shift in the redox potential. The remarkable peak separation on Ag–Cu@ZnO-NFLC/GCE could be explained by its larger surface area, which facilitates electron transfer and increases adsorption strength toward biomolecules.

The plot of scan rate *vs* peak current density shows that the linear regression equation for the oxidation and reduction of peak currents is Ip_a (mA) = 0.03987 ν (mV s^{-1}) + 0.00024, R^2 = 0.99 Ipc (μA) = −0.00391ν (mV s^{-1}) − 0.00031, R^2 = 0.98, respectively, as depicted in Fig. 4c. This linearity implies the role of the surface-controlled process in its electrochemical kinetics. However, the Randles–Sevcik equation was used to calculate the diffusion coefficient of DA for the bare GCE and Ag–Cu@ZnO/GCE using eqn (1).

$$I_p = (2.69 \times 10^5) n^{3/2} A D^{1/2} C \nu^{1/2} \quad (1)$$

Here, A is the electrode surface area, n is the number of electrons transferred, ν is the scan rate, D is the diffusion coefficient, I_p is the peak current and C is the concentration of DA calculated from the above equation. The D values for Ag–Cu@ZnO/GCE and GCE were

© 2021 The Author(s). Published by the Royal Society of Chemistry

Open Access Article. Published on 28 July 2021. Downloaded on 7/28/2025 10:24:16 PM.
This article is licensed under a Creative Commons Attribution-NonCommercial 3.0 Unported Licence.

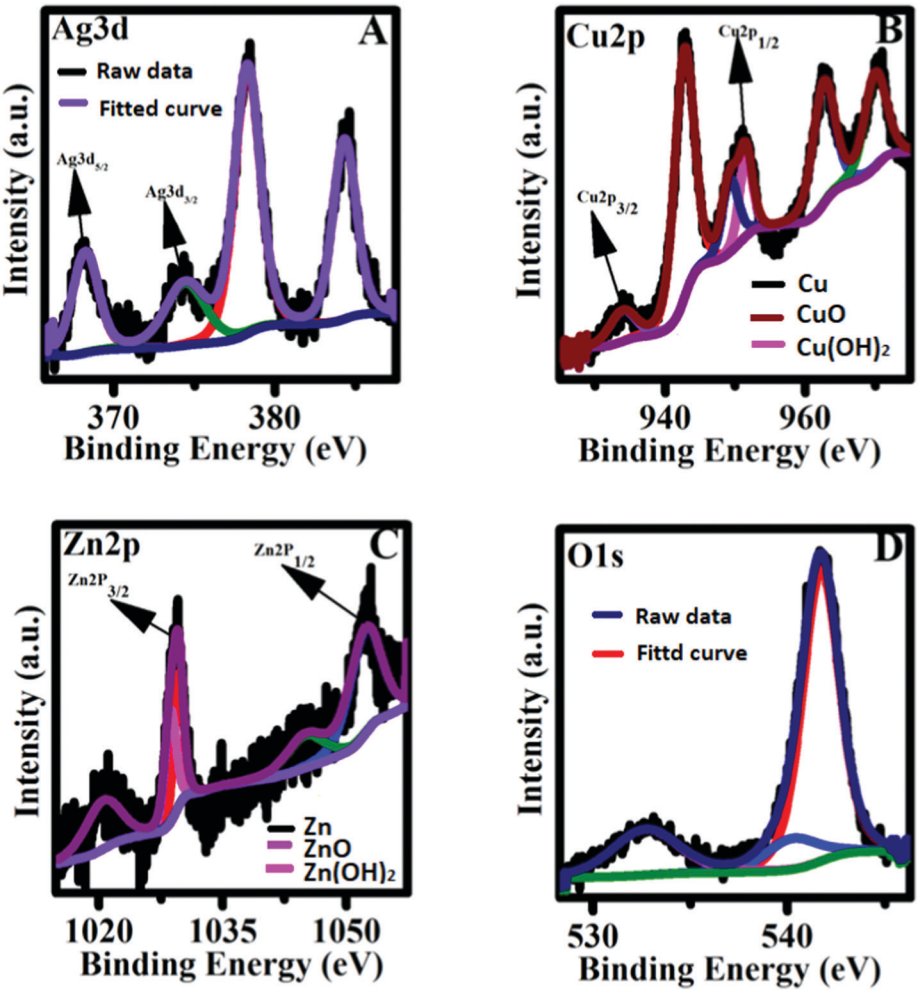

Fig. 3 XPS spectra of (A) Ag3d, (B) Cu2p, (C) Zn2p, and (D) O1s.

determined to be 7.496×10^{-6} cm^2 s^{-1} and 14.136×10^{-6} cm^2 s^{-1}, respectively, and these improved D values may be correlated with the higher electrochemical active surface area for the Ag–Cu@ZnO-NFLC modified GCE compared to the bare GCE. Chronocoulometry (CC) is used to readily determine the real electrochemical active electrode area, as well as their respective diffusion coefficients, the time-window of an electrochemical cell and the adsorption of electroactive species.[37] The result demonstrated a reversible reaction with an active area of 0.072 cm^2. As shown in Fig. S2 (ESI†), the optimized amount of the material drop coated on the electrode surface was determined to be 1 mg mL^{-1}.

3.2.2. Studies with amperometric *i–t* curve and differential pulse voltammetry (DPV). DPV was performed in 0.1 M PBS for different concentrations of DA varying from 10 to 200 μM to study the oxidation and reduction behavior of DA at the modified GCE depicted in Fig. 5a.

It could be emphasized that the changes in the currents are insignificant for different concentrations of DA varying from 10 to 200 μM, which indicates the stability of the Ag–Cu@ZnO NFLC modified GCE composite electrode. Based on the result, it is obvious that the formed Ag–Cu on ZnO is highly stable and active and it is a suitable catalytic electrode for electrochemical redox reactions.[40]

However, in order to formulate the mathematical relation between the voltammetric current response of Ag–Cu@ZnO-NFLC/GCE and DA concentration, a calibration curve has been established for the understanding of the curve depicted in Fig. 5b. The DPV studies clearly showed that the I_p is linear with DA concentration with an enhanced high sensitivity of I (mA) = 0.0291c (mA mM^{-1}) + 0.00033 (R^2 = 0.99) over a low limit of detection of 0.21 μM and a sensitivity of 0.68 μA μM^{-1} cm^{-2}.

3.2.3. Studies on the effect of pH in the electrochemical response of DA on the Ag–Cu@ZnO-NFLC/GCE sensor. The pH experiments on the ZnO nanoflower-like composite-modified GCE electrode have resulted in the electrochemical response of DA on the GCE electrode at pH values ranging from 4.0 to 9.0 in 0.1 M PBS solution consisting of 100 μM DA, as shown in Fig. 5c.

Fig. 5c shows that the oxidation peak current will increase with an increase in the solution pH from 4.0 to 9.0 and, henceforth, diminishes with a further increase in pH, illustrating the inclusion of protons within the electrode reaction

Open Access Article. Published on 28 July 2021. Downloaded on 7/28/2025 10:24:16 PM.
This article is licensed under a Creative Commons Attribution-NonCommercial 3.0 Unported Licence.

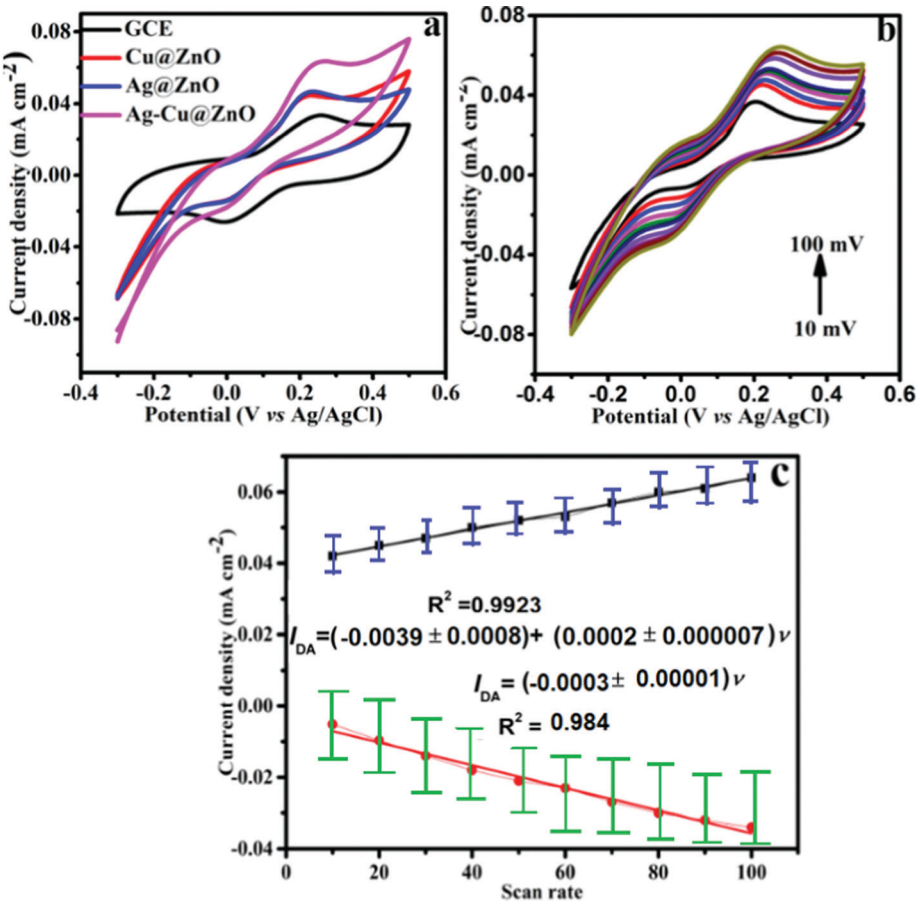

Fig. 4 (a) Cyclic voltammograms of the bare GCE, Cu@ZnO, Ag@ZnO and Ag–Cu@ZnO NFLC modified GCE in 0.1 M PBS (pH = 7.0) with 100 μM DA. Scan rate: 50 mV s^{-1}. (b) Cyclic voltammograms of 100 μM DA on the Ag–Cu@ZnO modified GCE at different scan rates in 0.1 M PBS (pH = 7.0). (c) Plot of the redox peak current *versus* scan rate.

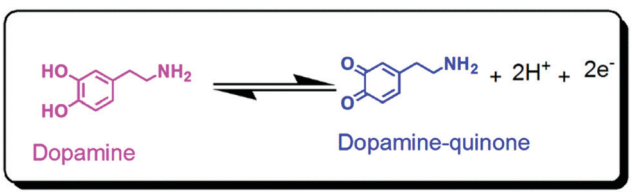

Scheme 1 Oxidation of dopamine to dopamine-quinone and its reduction to DA.

processes, leading to a maximum pH. A large amount of hydroxyl ions perhaps uproot DA on the surface assimilation sites of the Au–Cu@ZnO nanoflower-like composite surface. After the pH of the solution is reduced below the pK_a value (9.8), the DA resides in a non-dissociated form. Afterwards, it exists as associated ions at a higher pH, leading to a lower current. The non-dissociated DA may be more adsorbed on the electrode surface than the dissociated DA, resulting in the most extreme current response at a lower pK_a value.

Since the electrochemical oxidation of DA includes deprotonation, the electrode reaction diminishes under acidic conditions leading to a reduction of peak currents. The pH of 7.0 is consistently chosen for the initial analytical experiments.

Fig. 6a depicts the amperometric *i–t* responses recorded for different DA concentrations in the range of 0.1–10 μM at the Ag–Cu@ZnO-NFLC/GCE. An applied potential of 0.24 V was maintained between the Ag–Cu@ZnO-NFLC/GCE and the Ag/AgCl reference electrode in the amperometric *i–t* experiment, in 0.1 M PBS solution, with a continuous addition of 1 M DA.

The samples were spiked in order to record the current responses of the fabricated nanocomposite electrode. Simultaneously, the DA concentration was enhanced from 0.1 to 10 μM. The amperometric current response of the fabricated nanocomposite electrode showed a rapid response to DA from the amperometric *i–t* curve. The response time for the rapid detection of DA is calculated to be 3 seconds, which is one of the attributes of a DA sensor for the quick detection of DA in real-time samples. Fig. 6b represents the calibration curve established between the amperometric current responses and various concentrations of DA. The figure shows a linear plot with a high sensitivity of I (mA) = 0.0475c mA μM^{-1} + 0.00241 (R^2 = 0.99) from 0.1 to 10 μM at a low detection limit and higher sensitivities of 0.228 μM and 0.72 μA μM^{-1} cm^{-2}.

3.2.4. Studies on the stability, interference and reproducibility of the Ag–Cu@ZnO-NFLC/GCE sensor. Amperometric current responses for human urine samples were recorded to

© 2021 The Author(s). Published by the Royal Society of Chemistry

Open Access Article. Published on 28 July 2021. Downloaded on 7/28/2025 10:24:16 PM.
This article is licensed under a Creative Commons Attribution-NonCommercial 3.0 Unported Licence.

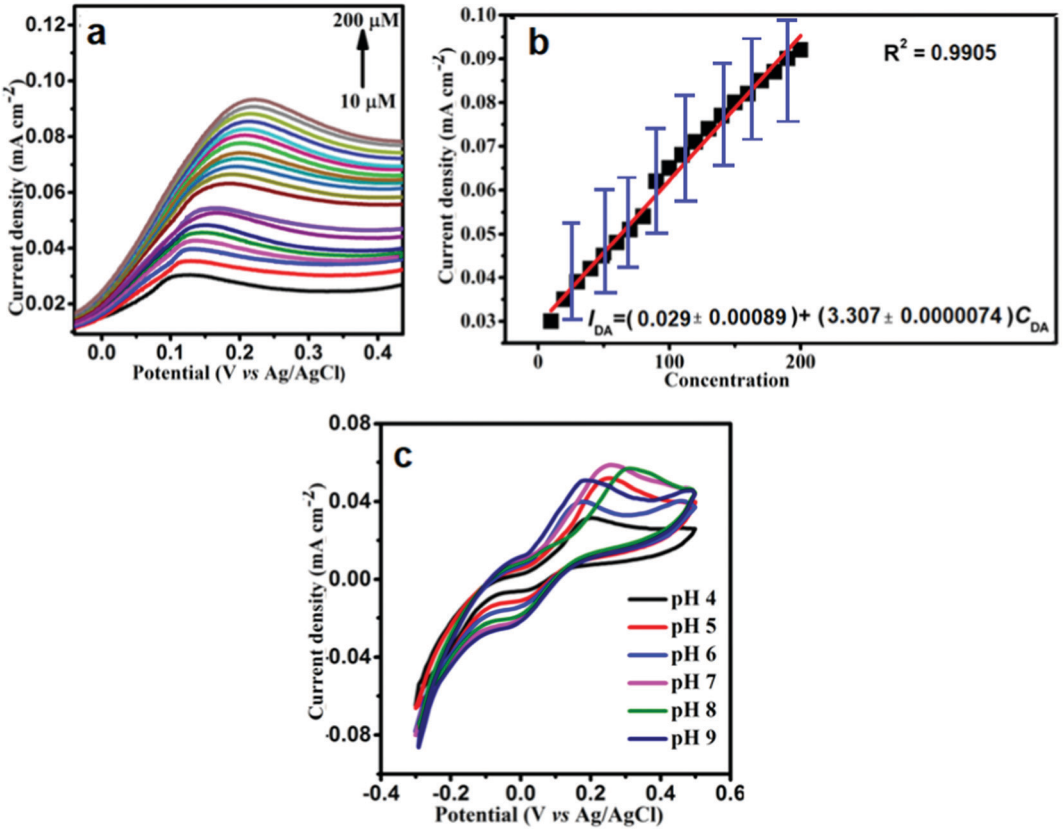

Fig. 5 (a) Differential pulse voltammetry curves of the Ag–Cu@ZnO NFLC modified GCE in 0.1 M PBS (pH = 7.0) containing 10–200 μM DA. (b) The corresponding plot of the oxidation peak current of DA *vs.* DA concentration for differential pulse voltammetry measurements. (c) Cyclic voltammograms of the Ag–Cu@ZnO NFLC modified GCE in 0.1 M PBS with different pH values containing 100 μM DA at a scan rate of 50 mV s^{-1}.

study the analytical capability of the proposed flower-like nanocomposite modified GCE electrode. The collected human urine sample was added directly to the 0.1 M PBS (pH 7.0) and an applied potential of 0.24 V was used between the fabricated working electrode and the Ag/AgCl reference electrode. Fig. 6c shows an increased current response which was observed when the urine sample was spiked with known concentrations of DA continuously at a regular interval of time, that is, 250 seconds. Then, the corresponding detected DA concentrations from the amperometric current responses were 0.030 μM, 0.052 μM and 0.070 μM, respectively, from 1 μM of the urine sample. All these results indicate that the fabricated nanocomposite electrode has the analytical capability to detect DA in human urine samples rapidly with high sensitivity and selectivity. However, for studying the intra- and inter-assay of the fabricated nanoflower-like composite electrode, 12 fabricated working electrodes were taken and were immersed in 0.1 M PBS (pH 7.0) containing 0.1 μM DA. Eventually, their amperometric current responses were recorded. The relative standard deviation observed for intra- and inter-assay was estimated to be 2.3 and 2.6%, respectively, indicating that the fabrication protocol adopted for the construction of Ag–Cu@ZnO NFLC/GCE is stable and reliable. In addition, the stability of Ag–Cu@ZnO NFLC/GCE was also investigated by subjecting it to 1 μM DA for a period of 15 days, and the recorded amperometric current response was stable for this 15-day period of time. Furthermore, there was no substantial change in the amperometric current response during the stability study of 15 days. These recorded observations indicate that the proposed sensor was stable. In this selectivity study, organic compounds and inorganic ions (0.02 mM of uric acid, ascorbic acid, caffeic acid, endorphin, phenethylamine, histamine, acetylcholine, serotonin, *etc.*) were used as potential interfering species capable of interrupting the amperometric signal response for DA. Hence, these results indicate that the proposed Ag–Cu@ZnO nanoflower-like composite electrode can be used to monitor real-time sample analysis and another predominant factor is that the results do not exhibit any significant interference signals, compared to the *i–t* current response of 0.1 μM DA. This indicates the excellent selectivity of the modified electrode towards DA.

However, the performance of the developed DA sensor in the present work can be compared with the other existing ZnO-based DA sensors in Table 1, and Table S1 (ESI†) shows the comparison of the proposed Ag–Cu@ZnO nanoflower-like composite DA sensor with other nanomaterial/composite sensors. The data required for the tabular representation of the recorded sensitivities were obtained from previously reported studies, and Table 1 and Table S1 (ESI†) are evident that the fabricated electrode material may be used for magnificent sensing abilities with respect to better linear ranges, lowest limits of detection and high sensitivities in contrast to alternately modified electrodes. Perhaps, this is associated

Open Access Article. Published on 28 July 2021. Downloaded on 7/28/2025 10:24:16 PM.
This article is licensed under a Creative Commons Attribution-NonCommercial 3.0 Unported Licence.

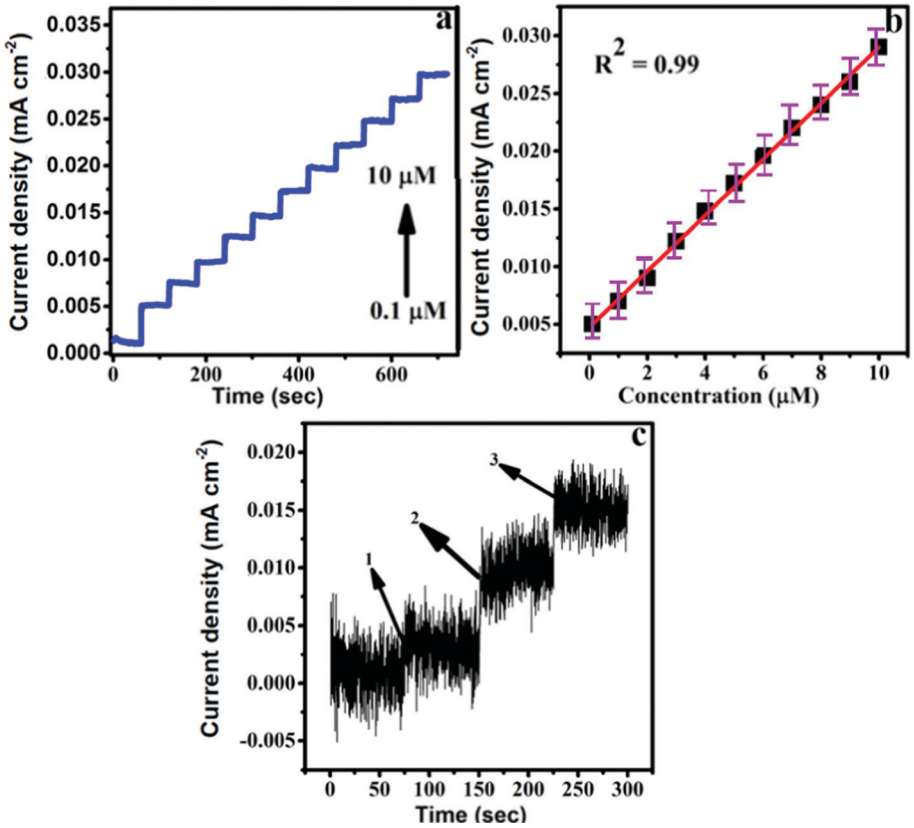

Fig. 6 (a) A typical amperometric curve obtained for Ag–Cu@ZnO modified GCE in 0.1 M PBS (pH = 7.0) at 0.24 V. (b) The corresponding calibration plot with the concentration of DA varying between 0.1 and 10 μM. (c) Amperometric response of an Ag–Cu@ZnO NFLC modified GCE after the subsequent addition of (1) 0.030, (2) 0.052, (3) and 0.070 μM DA in the presence of 1 μM of urine sample.

with the excellent conductivity and enhanced surface area of the fabricated electrode material. Apart from this, the material synthesis involves a low-cost and rapid single-step synthesis strategy through which Ag–Cu@ZnO nanoflower-like composites are obtained.

4. Conclusion

In this study, an Ag–Cu@ZnO nanoflower-like composite was synthesized using a simple, low-cost, fast single-step synthesis process, which was drop cast onto a GCE for DA electrochemical detection. The Ag–Cu@ZnO-NFLC/GCE findings revealed promising and improved electrochemical detection of DA, with excellent sensitivity and low detection limits. The Ag–Cu@ZnO-NFLC/GCE sensor showed a significant increase in oxidation peak currents, indicating that the as-prepared Ag–Cu@ZnO-NFLC/GCE sensor may be utilized as an electrochemical sensor for fast detection of DA. Furthermore, the Ag–Cu@ZnO-NFLC/GCE showed excellent stability, repeatability, and anti-interference properties. The Ag–Cu nanocomposite material provides enhanced support for the adsorption of DA and also helps in the mobility of the electrons between the GCE and the analyte, henceforth exhibiting a remarkable increase in the electron transfer rate. When compared to the GCE and Ag@ZnO and Cu@ZnO nanocomposite samples, the remarkable increase in the redox peak currents at the Ag–Cu@ZnO-NFLC/GCE with a properly defined redox pair of dopamine enables it to show greater electrocatalytic activity. Overall, the synthesis technique used is simple and cost-effective, making this sensor material ideal for the production of low-cost sensors with excellent stability and efficiency.

Conflicts of interest

The authors declare no competing interest.

Acknowledgements

This manuscript is dedicated to in loving memory of (late) Prof. Korupolu Raghu Babu-Andhra University College of Engineering, Visakhapatnam, India. Authors, Srikanth Ponnada and Prof. Annapurna Nowduri, would like to thank Andhra University College of Engineering, Visakhapatnam, India, the Indian Institute of Science, Bangalore, India, IIT Jodhpur, India, and University Grants Commission, India, for resource and technical support. Demudu Babu Gorle would like to thank the Indian Institute of Science, Bangalore, India, Andhra University College of Engineering, Visakhapatnam, India, University Grants Commission, and Government of India for providing Dr D. S. Kothari postdoctoral fellowship. Maryam Sadat Kiai would like to thank Istanbul Technical University, Istanbul, and Andhra University College of Engineering, Visakhapatnam, India. Saravanakumar Rajagopal would like to thank Anna University, Chennai, India, and Andhra University College of Engineering,

© 2021 The Author(s). Published by the Royal Society of Chemistry

Visakhapatnam, India. Prof. Rakesh Kumar Sharma gratefully acknowledges SERB-CRG/2020/002163.

Open Access Article. Published on 28 July 2021. Downloaded on 7/28/2025 10:24:16 PM. This article is licensed under a Creative Commons Attribution-NonCommercial 3.0 Unported Licence.

References

1 Z. Wang, H. Guo, R. Gui, H. Jin, J. Xia and F. Zhang, Simultaneous and selective measurement of dopamine and uric acid using glassy carbon electrodes modified with a complex of gold nanoparticles and multiwall carbon nanotubes, *Sens. Actuators, B*, 2018, **255**, 2069–2077.

2 Y. Pang, Y. Shi, Y. Pan, Y. Yang, Y. Long and H. Zheng, Facile and sensitive detection of dopamine based on in situ formation of fluorescent polydopamine nanoparticles catalyzed by peroxidase-like ficin, *Sens. Actuators, B*, 2018, **263**, 177–182.

3 A. J. Wang, J. J. Feng, W. J. Dong, Y. H. Lu, Z. H. Li and M. L. Riekkola, Spermine-*graft*-dextran non-covalent copolymer as coating material in separation of basic proteins and neurotransmitters by capillary electrophoresis, *J. Chromatogr. A*, 2010, **1217**(31), 5130–5136.

4 F. Gao, L. Liu, G. Cui, L. Xu, X. Wu, H. Kuang and C. Xu, Regioselective plasmonic nano-assemblies for bimodal sub-femtomolar dopamine detection, *Nanoscale*, 2017, **9**(1), 223–229.

5 K. E. Hubbard, A. Wells, T. S. Owens, M. Tagen, C. H. Fraga and C. F. Stewart, Determination of dopamine, serotonin, and their metabolites in pediatric cerebrospinal fluid by isocratic high performance liquid chromatography coupled with electrochemical detection, *Biomed. Chromatogr.*, 2010, **24**, 626–631.

6 A. Özcan, S. İlkbaş and A. A. Özcan, Development of a disposable and low-cost electrochemical sensor for dopamine detection based on poly (pyrrole-3-carboxylic acid)-modified electrochemically over-oxidized pencil graphite electrode, *Talanta*, 2017, **165**, 489–495.

7 R. Gupta, P. K. Rastogi, V. Ganesan, D. K. Yadav and P. K. Sonkar, Gold nanoparticles decorated mesoporous silica microspheres: a proficient electrochemical sensing scaffold for hydrazine and nitrobenzene, *Sens. Actuators, B*, 2017, **239**, 970–978.

8 L. Wang, Y. Zheng, X. Lu, Z. Li, L. Sun and Y. Song, Dendritic copper-cobalt nanostructures/reduced graphene oxide-chitosan modified glassy carbon electrode for glucose sensing, *Sens. Actuators, B*, 2014, **195**, 1–7.

9 M. Baghayeri, H. Veisi, S. Farhadi, H. Beitollahi and B. Maleki, Ag nanoparticles decorated Fe 3 O 4/chitosan nanocomposite: synthesis, characterization and application toward electrochemical sensing of hydrogen peroxide, *J. Iran. Chem. Soc.*, 2018, **15**(5), 1015–1022.

10 D. Sharma, M. I. Sabela, S. Kanchi, K. Bisetty, A. A. Skelton and B. Honarparvar, Green synthesis, characterization and electrochemical sensing of silymarin by ZnO nanoparticles: experimental and DFT studies, *J. Electroanal. Chem.*, 2018, **808**, 160–172.

11 J. Lee, O. K. Farha, J. Roberts, K. A. Scheidt, S. T. Nguyen and J. T. Hupp, Metal–organic framework materials as catalysts, *Chem. Soc. Rev.*, 2009, **38**(5), 1450–1459.

12 A. A. Firooz, M. Ghalkhani, J. A. F. Albanese and M. Ghanbari, High electrochemical detection of dopamine based on Cu doped single phase hexagonally ZnO plates, *Mater. Today Commun.*, 2020, 101716.

13 N. Baig, A. N. Kawde and M. Ibrahim, Efficient ionic medium supported reduced graphene oxide-based sensor for selective sensing of dopamine, *Mater. Adv.*, 2020, **1**(4), 783–793.

14 F. Gao, T. Fan, S. Ou, J. Wu, X. Zhang, J. Luo, N. Li, Y. Yao, Y. Mou, X. Liao and D. Geng, Highly efficient electrochemical sensing platform for sensitive detection DNA methylation, and methyltransferase activity based on Ag NPs decorated carbon nanocubes, *Biosens. Bioelectron.*, 2018, **99**, 201–208.

15 Y. Dong, C. Duan, Q. Sheng and J. Zheng, Preparation of Ag@zeolitic imidazolate framework-67 at room temperature for electrochemical sensing of hydrogen peroxide, *Analyst*, 2019, **144**(2), 521–529.

16 F. Qu, H. Lu, M. Yang and C. Deng, Electrochemical immunosensor based on electron transfer mediated by graphene oxide initiated silver enhancement, *Biosens. Bioelectron.*, 2011, **26**(12), 4810–4814.

17 S. Drexler, J. Faria, M. P. Ruiz, J. H. Harwell and D. E. Resasco, Amphiphilic nanohybrid catalysts for reactions at the water/oil interface in subsurface reservoirs, *Energy Fuels*, 2012, **26**(4), 2231–2241.

18 A. Anaraki Firooz and M. Keyhani, The Effect of Different Dopants (Cr, Mn, Fe, Co, Cu and Ni) on Photocatalytic Properties of ZnO Nanostructures. International, *J. Nanosci. Nanotechnol.*, 2020, **16**(1), 59–65.

19 R. Ahmad, N. Tripathy, M. S. Ahn, K. S. Bhat, T. Mahmoudi, Y. Wang, J. Y. Yoo, D. W. Kwon, H. Y. Yang and Y. B. Hahn, Highly efficient non-enzymatic glucose sensor based on CuO modified vertically-grown ZnO nanorods on electrode, *Sci. Rep.*, 2017, **7**(1), 1–10.

20 K. Khun, Z. H. Ibupoto, X. Liu, N. A. Mansor, A. P. F. Turner, V. Beni and M. Willander, An electrochemical dopamine sensor based on the ZnO/CuO nanohybrid structures, *J. Nanosci. Nanotechnol.*, 2014, **14**(9), 6646–6652.

21 X. Zhang, Y. C. Zhang and L. X. Ma, One-pot facile fabrication of graphene-zinc oxide composite and its enhanced sensitivity for simultaneous electrochemical detection of ascorbic acid, dopamine and uric acid, *Sens. Actuators, B*, 2016, **227**, 488–496.

22 J. Lin, B. Huang, Y. Dai, J. Wei and Y. Chen, Chiral ZnO nanoparticles for detection of dopamine, *Mater. Sci. Eng., C*, 2018, **93**, 739–745.

23 Y. Song, J. Han, L. Xu, L. Miao, C. Peng and L. Wang, A dopamine-imprinted chitosan Film/Porous ZnO NPs@ carbon Nanospheres/Macroporous carbon for electrochemical sensing dopamine, *Sens. Actuators, B*, 2019, **298**, 126949.

24 C. Yang, C. Zhang, T. Huang, X. Dong and L. Hua, Ultra-long ZnO/carbon nanofiber as free-standing electrochemical

Open Access Article. Published on 28 July 2021. Downloaded on 7/28/2025 10:24:16 PM.
This article is licensed under a Creative Commons Attribution-NonCommercial 3.0 Unported Licence.

sensor for dopamine in the presence of uric acid, *J. Mater. Sci.*, 2019, **54**(24), 14897–14904.

25 M. Zhao, Z. Li, X. Zhang, J. Yu, Y. Ding, H. Li and Y. Ma, Employing the interfacial barrier of P-rGO/ZnO microspheres for improving the electrochemical sensing performance to dopamine, *Sens. Actuators, B*, 2020, **309**, 127757.

26 A. A. Firooz, M. Ghalkhani, J. A. F. Albanese and M. Ghanbari, High electrochemical detection of dopamine based on Cu doped single phase hexagonally ZnO plates, *Mater. Today Commun.*, 2020, 101716.

27 H. Y. Yue, H. J. Zhang, S. Huang, X. X. Lu, X. Gao, S. S. Song, Z. Wang, W. Q. Wang and E. H. Guan, Highly sensitive and selective dopamine biosensor using Au nanoparticles-ZnO nanocone arrays/graphene foam electrode, *Mater. Sci. Eng., C*, 2020, **108**, 110490.

28 L. Zhihua, Z. Xue, H. Xiaowei, Z. Xiaobo, S. Jiyong, X. Yiwei, H. Xuetao, S. Yue and Z. Xiaodong, Hypha-templated synthesis of carbon/ZnO microfiber for dopamine sensing in pork, *Food Chem.*, 2021, **335**, 127646.

29 S. Kogularasu, M. Akilarasan, S. M. Chen, T. W. Chen and B. S. Lou, Urea-based morphological engineering of ZnO; for the biosensing enhancement towards dopamine and uric acid in food and biological samples, *Mater. Chem. Phys.*, 2019, **227**, 5–11.

30 X. Zhang and J. Zheng, Hollow carbon sphere supported Ag nanoparticles for promoting electrocatalytic performance of dopamine sensing, *Sens. Actuators, B*, 2019, **290**, 648–655.

31 Y. Y. Li, P. Kang, S. Q. Wang, Z. G. Liu, Y. X. Li and Z. Guo, Ag nanoparticles anchored onto porous CuO nanobelts for the ultrasensitive electrochemical detection of dopamine in human serum, *Sens. Actuators, B*, 2021, **327**, 128878.

32 C. Zhang, Z. Cao, G. Zhang, Y. Yan, X. Yang, J. Chang, Y. Song, Y. Jia, P. Pan, W. Mi and Z. Yang, An electrochemical sensor based on plasma-treated zinc oxide nanoflowers for the simultaneous detection of dopamine and diclofenac sodium, *Microchem. J.*, 2020, **158**, 105237.

33 S. Ghosh, R. Das, I. H. Chowdhury, P. Bhanja and M. K. Naskar, Rapid template-free synthesis of an air-stable hierarchical copper nanoassembly and its use as a reusable catalyst for 4-nitrophenol reduction, *RSC Adv.*, 2015, **5**(123), 101519–101524.

34 H. Y. Niu, S. L. Liu, Y. Q. Cai, F. C. Wu and X. L. Zhao, MOF derived porous carbon supported Cu/Cu2O composite as high performance non-noble catalyst, *Microporous Mesoporous Mater.*, 2016, **219**, 48–53.

35 I. Najdovski, P. R. Selvakannan and A. P. O'Mullane, Electrochemical formation of Cu/Ag surfaces and their applicability as heterogeneous catalysts, *RSC Adv.*, 2014, **4**(14), 7207–7215.

36 M. Konsolakis, S. A. C. Carabineiro, E. Papista, G. E. Marnellos, P. B. Tavares, J. A. Moreira, Y. Romaguera-Barcelay and J. L. Figueiredo, Effect of preparation method on the solid state properties and the deN(2)O performance of CuO–CeO 2 oxides, *Catal. Sci. Technol.*, 2015, **5**(7), 3714–3727.

37 A. García-Miranda Ferrari, C. W. Foster, P. J. Kelly, D. A. Brownson and C. E. Banks, Determination of the electrochemical area of screen-printed electrochemical sensing platforms, *Biosensors*, 2018, **8**(2), 53.

38 A. A. Firooz, M. Ghalkhani, J. A. F. Albanese and M. Ghanbari, High electrochemical detection of dopamine based on Cu doped single phase hexagonally ZnO plates, *Mater. Today Commun.*, 2021, **26**, 101716.

39 H. Y. Yue, H. J. Zhang, S. Huang, X. X. Lu, X. Gao, S. S. Song, Z. Wang, W. Q. Wang and E. H. Guan, Highly sensitive and selective dopamine biosensor using Au nanoparticles-ZnO nanocone arrays/graphene foam electrode, *Mater. Sci. Eng., C*, 2020, **108**, 110490.

40 D. B. Gorle and M. A. Kulandainathan, Electrochemical sensing of dopamine at the surface of a dopamine grafted graphene oxide/poly (methylene blue) composite modified electrode, *RSC Adv.*, 2016, **6**(24), 19982–19991.

41 G. Nagaraju, S. A. Prashanth, M. Shastri, K. V. Yathish, C. Anupama and D. Rangappa, Electrochemical heavy metal detection, photocatalytic, photoluminescence, biodiesel production and antibacterial activities of Ag–ZnO nanomaterial, *Mater. Res. Bull.*, 2017, **94**, 54–63.

42 K. Lefatshe, C. M. Muiva and L. P. Kebaabetswe, Extraction of nanocellulose and in-situ casting of ZnO/cellulose nanocomposite with enhanced photocatalytic and antibacterial activity, *Carbohydr. Polym.*, 2017, **164**, 301–308.

43 K. A. Kumar, B. Lakshminarayana, D. Suryakala and C. Subrahmanyam, Reduced graphene oxide supported ZnO quantum dots for visible light-induced simultaneous removal of tetracycline and hexavalent chromium, *RSC Adv.*, 2020, **10**(35), 20494–20503.

44 W. Muhammad, N. Ullah, M. Haroon and B. H. Abbasi, Optical, morphological and biological analysis of zinc oxide nanoparticles (ZnO NPs) using Papaver somniferum L, *RSC Adv.*, 2019, **9**(51), 29541–29548.

45 N. Baig, I. Kammakakam and W. Falath, Nanomaterials: a review of synthesis methods, properties, recent progress, and challenges, *Mater. Adv.*, 2021, **2**(6), 1821–1871.

46 S. Ingavale, P. Marbaniang, B. Kakade and A. Swami, Starbon with Zn-N and Zn-O active sites: An efficient electrocatalyst for oxygen reduction reaction in energy conversion devices, *Catal. Today*, 2021, **370**, 55–65.

47 D. B. Gorle, S. Ponnada, M. S. Kiai, K. K. Nair, A. Nowduri, H. Swart, E. H. Ange and K. K. Nanda, Review on recent progress in metal-organic frameworks-based materials for fabricating electrochemical glucose sensors, *J. Mater. Chem. B*, 2021, DOI: 10.1039/D1TB01403J.

© 2021 The Author(s). Published by the Royal Society of Chemistry